

# Anisotropy induced Feshbach resonances in a quantum dipolar gas of magnetic atoms

Alexander Petrov,<sup>1</sup> Eite Tiesinga,<sup>2</sup> and Svetlana Kotochigova<sup>1,\*</sup>

<sup>1</sup>*Department of Physics, Temple University, Philadelphia, Pennsylvania 19122 and National Institute of Standards and Technology, Gaithersburg, Maryland 20899, USA<sup>†</sup>*  
<sup>2</sup>*Joint Quantum Institute, National Institute of Standards and Technology and University of Maryland, Gaithersburg, Maryland 20899, USA*

We explore the anisotropic nature of Feshbach resonances in the collision between ultracold magnetic submerged-shell dysprosium atoms, which can only occur due to couplings to rotating bound states. This is in contrast to well-studied alkali-metal atom collisions, where most Feshbach resonances are hyperfine induced and due to rotation-less bound states. Our novel first-principle coupled-channel calculation of the collisions between open-4f-shell spin-polarized bosonic dysprosium reveals a striking correlation between the anisotropy due to magnetic dipole-dipole and electrostatic interactions and the Feshbach spectrum as a function of an external magnetic field. Over a 20 mT magnetic field range we predict about a dozen Feshbach resonances and show that the resonance locations are exquisitely sensitive to the dysprosium isotope.

PACS numbers: 03.65.Nk, 31.10.+z, 34.50.-s

A strongly interacting quantum gas of magnetic atoms, placed in an optical lattice, provides the opportunity to examine strongly correlated matter, creating a platform to explore exotic many-body phases known in solids, quantum ferrofluids, quantum liquid crystals, and supersolids [1, 2]. Recent experimental advances [3–10] in trapping and cooling magnetic atoms pave the way towards these goals.

In general, interactions between magnetic atoms are orientationally dependent or anisotropic. At room temperature anisotropic interactions are much smaller than kinetic energies and other major interactions between atoms, therefore can be ignored. The situation is different for an ultracold gas of atoms with a large magnetic moment. It was, for example, demonstrated that the anisotropy due to magnetic dipole-dipole interactions between ultracold chromium atoms leads to an anisotropic deformation of a Bose Einstein condensate (BEC) [11]. Moreover, anisotropy plays a dominant role in collisional relaxation of ultracold atoms with large magnetic moments [5–7, 12–15].

In this Letter we pursue ideas for using anisotropic magnetic and dispersion interactions to control collisions of ultracold magnetic atoms by using Feshbach resonances [16]. Resonances, shown schematically in Fig. 1, appear when the energy of “embedded” bound states cross the energy of the entrance channel or initial scattering state. The embedded state is a level of a potential dissociating to a closed channel whose asymptotic energy is larger than that of the entrance channel. Coupling with the entrance channel leads to a resonance.

Feshbach resonances make it possible to convert a weakly interacting gas of atoms into one that is strongly interacting and along the way promise to make available many of the collective many-body states mentioned above. Alternatively, interactions can be turned off all together to create an ideal Fermi or Bose gas, for which

thermodynamic properties are known analytically. Feshbach resonances can also be used to create BECs of weakly-bound molecules [17], which can be optically stabilized to deeply-bound molecules [18]. For fermionic atoms the BCS-BEC phase transition [19] and universal many-body behavior of strongly interacting magnetic atoms can be studied via Feshbach resonances. Finally, three-body Efimov physics [20] can be explored.

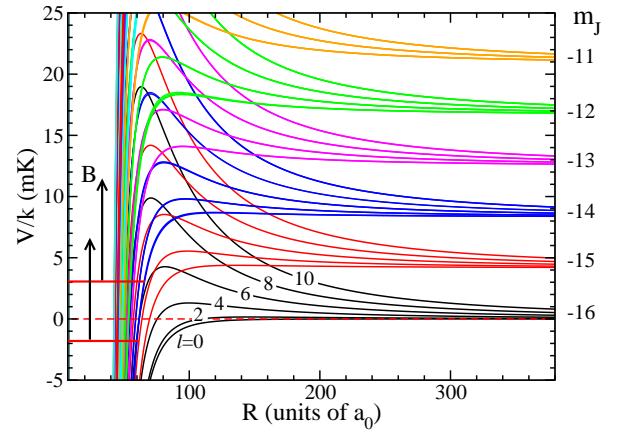


FIG. 1: (Color online) Potential energy curves for a  $^{164}\text{Dy}+^{164}\text{Dy}$  collision in an external magnetic field  $B$  as a function of internuclear separation. The (red) dashed line with zero energy indicates the energy of the entrance channel. Two Feshbach resonances are schematically shown by (red) horizontal lines, which end at the classical outer turning point of a closed channel. Their energy increases, indicated by arrows, with magnetic field and a resonance occurs when this energy equals the entrance-channel energy. There are 91 diagonal potential matrix elements for channels  $|j_1 j_2 j m_j, \ell m_\ell\rangle$  with  $m_j + m_\ell = -16$  and even  $\ell \leq 10$ . We use  $B = 50$  G. The curves are colored by their  $m_j$  value, while for  $m_j = -16$  curves their  $\ell$  value is indicated. Here  $1 \text{ G} = 0.1 \text{ mT}$ ,  $a_0 = 0.0529177 \text{ nm}$  is the Bohr radius, and  $k = 1.38065 \cdot 10^{-23} \text{ J/K}$  is the Boltzmann constant.

The most promising atoms to look for the effect of anisotropy on collisions are submerged-shell atoms, which have an electronic configuration with an unfilled inner shell shielded by a closed outer shell. In particular, we are interested in the rare-earth dysprosium (Dy) atom with a  $^5\text{I}_8$  ground-state, a total angular momentum  $j = 8$ , and a large magnetic moment of  $\approx 10\mu_B$ , for which the electron spins of the inner  $4f^{10}$  shell are aligned such that its orbital angular momentum is maximal and largely unquenched. Here  $\mu_B$  is the Bohr magneton. As a result, Dy's magnetic and electrostatic properties are highly anisotropic. A quantitative description of the collision between two dysprosium atoms is challenging. For example, our previous study [15] showed that there are 153 Born-Oppenheimer potentials that dissociate to the ground  $^5\text{I}_8 + ^5\text{I}_8$  state.

We present a first-principle coupled-channel model allowing us to calculate anisotropy-induced magnetic Feshbach-resonance spectra of bosonic Dy atoms. The model treats the Zeeman, magnetic dipole-dipole, and electrostatic isotropic and anisotropic dispersion interactions equally. Bosonic Dy isotopes have zero nuclear spin. Thus, there is no nuclear hyperfine structure and only Zeeman splittings remain. The weak quadrupole-quadrupole interaction [15] is included for completeness.

We already note that Feshbach resonances in rare-earth magnetic atoms are different in nature than those in alkali-metal atom collisions. As pointed out in Ref. [15] for a coupled-channel calculation there exists at most one channel with zero relative nuclear orbital angular momentum  $\vec{\ell}$ , which for ultra-cold collisions is also the entrance channel. Consequently, resonances occur due to anisotropic coupling to bound states with non-zero  $\ell$ .

The focus of this Letter is on ultra-cold collisions of atoms prepared in the energetically-lowest Zeeman state  $j = 8$  and projection  $m = -8$ . Inelastic exothermic atom-atom processes, where the spin projection of one or both of the atoms changes, are absent and, consequently, Feshbach resonances can be readily observed.

We start by setting up the Hamiltonian, interatomic potentials, and channel basis for two bosonic  $^5\text{I}_8$  Dy atoms with zero nuclear spin. This Hamiltonian assuming a magnetic field  $B$  along the  $\hat{z}$  direction is

$$H = -\frac{\hbar^2}{2\mu_r} \frac{d^2}{dR^2} + \frac{\vec{\ell}^2}{2\mu_r R^2} + H_Z + V(\vec{R}, \tau), \quad (1)$$

where  $\vec{R}$  describes the orientation of and separation between the two atoms. The first two terms are the radial kinetic and rotational energy operators, respectively. The Zeeman interaction is  $H_Z = g_s \mu_B (j_{1z} + j_{2z}) B$  with  $g_s = 1.24159$  the g-factor of Dy [21] and  $j_{iz}$  is the  $z$  component of the angular momentum operator  $\vec{j}_i$  of atom  $i = 1, 2$ . The electronic Hamiltonian, including nuclear repulsion,  $V(\vec{R}, \tau)$  is anisotropic and  $\tau$  labels the electronic variables. Finally,  $\mu_r$  is the reduced mass and for  $R \rightarrow \infty$  the interaction  $V(\vec{R}, \tau) \rightarrow 0$ .

Our coupled-channels calculations [22] are performed in the atomic basis  $|(j_1 j_2) j m_j, \ell m_\ell\rangle \equiv Y_{\ell m_\ell}(\theta, \phi) |(j_1 j_2) j m_j\rangle$ , where  $Y_{\ell m_\ell}(\theta, \phi)$  is a spherical harmonic and angles  $\theta$  and  $\phi$  give the orientation of the internuclear axis relative to the magnetic field direction. In this basis the Zeeman and rotational interaction are diagonal with energies  $g_s \mu_B m_j B + \hbar^2 \ell(\ell+1)/(2\mu_r R^2)$ . Coupling between the basis states is due to  $V(\vec{R}, \tau)$  and will be discussed in detail below. Excited atomic states, for example those with  $j_i \neq 8$ , are not included as their internal energy is sufficiently high that the effects of coupling to these states is negligible. The Hamiltonian  $H$  conserves  $M_{\text{tot}} = m_j + m_\ell$  and is invariant under the parity operation so that only even (odd)  $\ell$  are coupled. For homonuclear collisions only basis states with even  $j + \ell$  exist. Figure 1 shows an example of the long-range diagonal matrix elements in the atomic basis of the sum of the rotational, Zeeman, and electronic Hamiltonian. We have used  $M_{\text{tot}} = -16$  and even  $\ell \leq 10$ . In fact, only the potentials dissociating to the six energetically-lowest Zeeman states are shown. The large number of potentials indicates the large number of resonances that, in principle, are possible.

Coupling between basis states is due to  $V(\vec{R}, \tau)$ . It is convenient to first evaluate this operator in a molecular basis with body-fixed projection quantum numbers defined with respect to the internuclear axis. We use the molecular basis  $|(j_1 j_2) j \Omega\rangle$  with projection  $\Omega$  of  $\vec{j}$  along the internuclear axis. For  $\text{Dy}_2$  the matrix elements of  $V(\vec{R}, \tau)$  conserve the projection  $\Omega$  but not the length  $j$ . The eigenenergies of  $V(\vec{R}, \tau)$  at each value of  $R$  are the adiabatic (relativistic) Born-Oppenheimer potentials [23, 24]. Typically, these potentials  $U_{n|\Omega|\sigma}(R)$  are obtained from an electronic structure calculation and labeled by  $n|\Omega|_\sigma^\pm$ , where  $|\Omega|$  is the absolute value of  $\Omega$ ,  $\sigma = g/u$  is the *gerade/ungerade* symmetry of the electronic wavefunction, and  $n = 1, 2, \dots$  labels curves of the same  $|\Omega|_{g/u}^\pm$  in order of increasing energy. For bosonic  $\text{Dy}_2$  the 81 *gerade* states are superpositions of even  $j$ , while the 72 *ungerade* states are superpositions of odd  $j$ .

For  $R > 27a_0$ , beyond the Le Roy radius where the atomic electron clouds have negligible overlap, we assume that  $V(\vec{R}, \tau)$  is the sum of the magnetic dipole-dipole,  $V_{\mu\mu}(\vec{R}) \propto 1/R^3$ , the electric quadrupole-quadrupole,  $V_{QQ}(\vec{R}) \propto 1/R^5$ , and the van-der-Waals dispersion  $V_{\text{disp}}(\vec{R}) \propto 1/R^6$  interaction. Reference [15] reported the matrix elements of the operator  $V_{\text{disp}}(\vec{R})$  in the molecular basis and tabulated the adiabatic  $C_{6,n\Omega\sigma}$  dispersion coefficients obtained by diagonalizing  $V_{\text{disp}}(\vec{R})$ . Crucially, the eigenfunctions of  $V_{\text{disp}}(\vec{R})$  are independent of  $R$ .

At shorter range coupling between basis states is more complex. Rather than determining all Born-Oppenheimer potentials, we have opted for the following approach. First, we calculate the single *gerade* potential  $U_{16g}(R)$  with the maximal projection

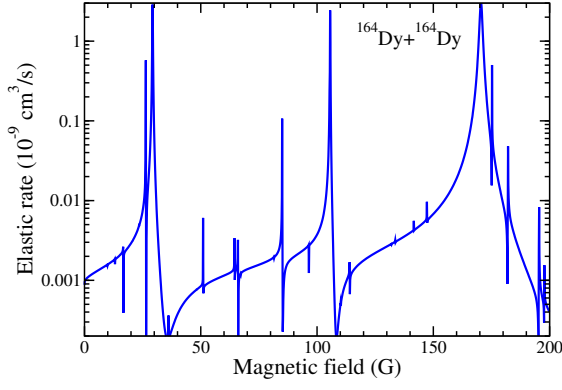


FIG. 2: Elastic rate coefficient of  $m = -8$   $^{164}\text{Dy}$  collisions as a function of magnetic field using a collision energy of  $E/k = 30$  nK. Partial waves  $\ell$  up to 10 are included.

$\Omega = 16$  using a coupled-cluster method with single, double, and perturbative triple excitations (CCSD(T)) [25] together with the scalar relativistic Stuttgart ECP28MWB pseudopotential and associated atomic bases sets (14s,13p,10d,8f,6g)/[10s8p5d4f3g]. The potential has a minimum at  $R_e = 8.771a_0$  with depth  $D_e/(hc) = 785.7 \text{ cm}^{-1}$ . For  $^{164}\text{Dy}_2$  it has a  $\omega_e/(hc) = 25.6 \text{ cm}^{-1}$  and contains 71 bound states. (We omit the  $n = 1$  label in  $U_{16g}(R)$ .) We then assume that the  $R < 27a_0$  electronic wavefunctions of the Born-Oppenheimer potentials are the same as those determined by the dispersion interaction, and the relation between energies of the *ab-initio* potentials is the same as for its  $C_6$  coefficient. Hence, the adiabatic potentials satisfy  $U_{n\Omega\sigma}(R)/U_{n'\Omega\sigma}(R) = C_{6,n\Omega\sigma}/C_{6,n'\Omega'\sigma}$  for  $R < 27a_0$  and with eigenfunctions as determined by the dispersion interaction. Equivalently, this allows us to write  $V(\vec{R}, \tau)$  in terms of  $U_{16g}(R)$  as

$$V(\vec{R}, \tau) = V_{\mu\mu}(\vec{R}) + V_{QQ}(\vec{R}) + \frac{U_{16g}(R)}{-C_{6,16g}/R^6} V_{\text{disp}}(\vec{R}) \quad (2)$$

for any  $R$ . This approach reduces the number of independent short-range potentials to one.

For practical reasons it is advantageous to write  $V_{\text{disp}}(\vec{R})$  as a sum of spherical tensor operators in the

TABLE I: Dispersion coefficients  $c_k^{(i)}$  in units of  $E_h a_0^6$ , where  $E_h = 4.35974 \times 10^{-18} \text{ J}$  is the Hartree. The strength of the magnetic dipole-dipole and quadrupole-quadrupole interaction are  $c_{\mu\mu} = -5.0269 \cdot 10^{-3} E_h a_0^3$  and  $c_{QQ} = 9.5719 \cdot 10^{-8} E_h a_0^5$ , respectively.

$k \setminus i$	1	2	3
0	-1873.4	$3.57 \cdot 10^{-3}$	$-6.82 \cdot 10^{-6}$
2	-0.1680	$5.06 \cdot 10^{-3}$	$-8.15 \cdot 10^{-6}$
4	$-6.56 \cdot 10^{-5}$		

laboratory frame. That is

$$V_{\text{disp}}(\vec{R}) = \frac{1}{R^6} \sum_{kq} \sum_i c_k^{(i)} (-1)^q C_{k,-q}(\theta, \phi) T_{kq}^{(i)}, \quad (3)$$

where  $C_{kq}(\theta, \phi) = \sqrt{4\pi/(2k+1)} Y_{kq}(\theta, \phi)$  and the spherical tensors  $T_{kq}^{(i)}$  of rank  $k$  and with components  $q$  are defined by

$$\begin{aligned} T_{00}^{(1)} &= I, & T_{2q}^{(1)} &= [j_1 \otimes j_1]_{2q} + [j_2 \otimes j_2]_{2q}, \\ T_{2q}^{(2)} &= [j_1 \otimes j_2]_{2q}, & T_{00}^{(2)} &= [j_1 \otimes j_2]_{00}, \\ T_{4q}^{(1)} &= [[j_1 \otimes j_1]_2 \otimes [j_2 \otimes j_2]_2]_{4q}, \\ T_{2q}^{(3)} &= [[j_1 \otimes j_1]_2 \otimes [j_2 \otimes j_2]_2]_{2q}, \\ T_{00}^{(3)} &= [[j_1 \otimes j_1]_2 \otimes [j_2 \otimes j_2]_2]_{00}, \end{aligned} \quad (4)$$

where  $I$  is the identity operator and  $[j \otimes j']_{kq}$  denotes a tensor product of angular momentum operators  $\vec{j}$  and  $\vec{j}'$  coupled to an operator of rank  $k$  and component  $q$  [26]. The higher-order tensor operators are constructed in an analogous manner. Equation 4 has three, three, and one tensors  $T_{kq}^{(i)}$  of rank  $k = 0, 2$ , and  $4$ , respectively. The dispersion coefficients  $c_k^{(i)}$ , listed in Table I, determine the strength of each term. Their order in Eq. 4 is by decreasing absolute value. The isotropic  $T_{00}^{(1)}$  term is the largest by far with the strongest anisotropic contribution from a dipolar (rank-2) operator constructed from the angular momentum of only one atom coupled to the rotation of the molecule. Finally, the magnetic dipole-dipole and quadrupole-quadrupole interaction are

$$V_{\mu\mu}(\vec{R}) = \frac{1}{R^3} c_{\mu\mu} \sum_q (-1)^q C_{2,-q}(\theta, \phi) T_{2q}^{(2)} \quad (5)$$

$$V_{QQ}(\vec{R}) = \frac{1}{R^5} c_{QQ} \sum_q (-1)^q C_{4,-q}(\theta, \phi) T_{4q}^{(1)}, \quad (6)$$

respectively. Their strengths are listed in Table I.

Figure 2 shows the elastic rate coefficient for the collision between two  $m = -8$   $^{164}\text{Dy}$  atoms at a collision energy of  $E/k = 30$  nK. We use  $M_{\text{tot}} = -16$  and include channels with even  $\ell$  up to ten leading to a close-coupling calculation with 91 channels. Fields up to  $B = 200$  G fall comfortably within the experimentally accessible values [16]. The graph shows a dozen of Feshbach resonances; some are broad, many are very narrow. By performing calculations that include fewer partial waves we have observed that the resonances can not be labeled by a single partial wave. For example, the three broad resonances at  $B \approx 30$  G, 110 G, and 170 G are already present when only  $\ell = 0, 2$ , and  $4$  channels are included. Their locations, however, shift significantly when higher  $\ell$  channels are included and only converge to within a few Gauss when  $\ell = 8$  channels are included. In general, we find that the magnetic-field location of a resonance that appears when channels with partial wave  $\ell$  are included stabilizes when channels up to  $\ell + 4$  are included.

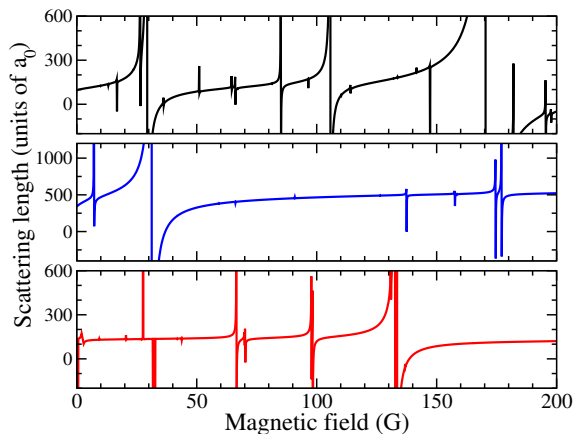


FIG. 3: Scattering length of  $m = -8$   $^{164}\text{Dy}$  atoms as a function of magnetic field with and without the magnetic dipole-dipole or the anisotropic contribution of the dispersion interaction. The top panel shows the case when all interactions are included. At  $B = 0$  the scattering length is  $89a_0$ . The middle and bottom panels are obtained when the dispersion and magnetic dipole-dipole anisotropy is set to zero, respectively. Even waves  $\ell$  up to 10 are included.

We stress that this behavior with increasing number of channels is unlike that observed in alkali-metal atom collisions [16] or even in collisions of strongly magnetic chromium atoms [27]. For these atoms resonances do not shift by more than a few Gauss when additional partial waves are added. Hence, resonances can be labeled by a partial wave quantum number. For dysprosium the anisotropic interactions are so strong that states with different partial waves are strongly mixed. We have also studied the effect of the uncertainty in the depth of the  $\Omega = 16$  Born-Oppenheimer potential. The depth  $D_e$  was changed by adding a localized correction to  $U_{16g}(R)$  that does not modify its long-range potential. A depth change by no more than  $10 \text{ cm}^{-1}$  changes its number of bound states by one. Changing the depth by smaller amounts changes the resonance spectrum non-trivially. For example resonance widths can be modified dramatically and rate coefficients with broad resonances that appear when  $d$ -wave channels are included can be observed.

The precise form of short-range potential and dispersion coefficients are not known. A few percent uncertainty is not unrealistic. For this Letter we have constructed potentials that lead to a positive  $B = 0$  scattering length  $a$  for  $^{164}\text{Dy}$  atoms in the  $m = -8$  state. This choice is suggested by the recent observation of a Bose condensed gas of  $^{164}\text{Dy}$  atoms at nearly zero magnetic field. It thus possesses a positive scattering length at this field [8]. Moreover, we chose the scattering length to be approximately equal to the mean scattering length [28] for (fictitious) scattering of a van der Waals potential with a  $C_6$  coefficient equal to the isotropic dispersion coefficient.

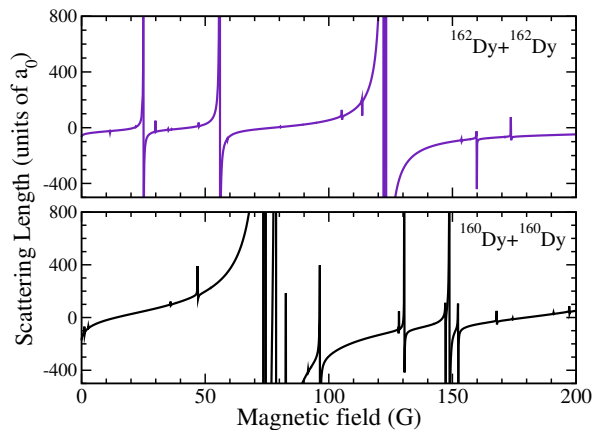


FIG. 4: Scattering length as a function of magnetic field for the bosonic isotopes  $^{162}\text{Dy}$  (top panel) and  $^{160}\text{Dy}$  (bottom panel). The magnetic state and number of included  $\ell$  is as in Fig. 3.

To further elucidate the effect of anisotropy, Fig. 3 shows the scattering length of  $m = -8$   $^{164}\text{Dy}$  collisions as a function of magnetic field when parts of the anisotropy are turned off. The top panel displays the case when all interactions are included corresponding to the elastic scattering described in Fig. 2. The bottom two panels show the effect of turning off the anisotropy in the dispersion and magnetic dipole-dipole interaction, respectively. The resonance spectra in the three panels are quite distinct. The number of resonances differs and, with one exception, the resonances are narrower.

Finally, Fig. 4 illustrates the effect of changing to different bosonic Dy isotopes. Since to good approximation Born-Oppenheimer potentials do not depend on the isotope, we have solved the coupled-channels equations using the appropriate reduced mass  $\mu_r$ . This observation has been used in understanding relationships between scattering lengths of isotopic combinations of spin-less ytterbium [29], while its limitations for Lithium Feshbach resonances have been studied in Ref. [30]. The field dependence of the scattering length changes from  $^{160}\text{Dy}$  to the  $^{162}\text{Dy}$  isotope. Measurement of resonance locations in different isotopes will be invaluable in understanding the scattering of dysprosium.

*Conclusion.* Applying a full coupled-channels calculation for ultracold atom-atom collisions, we have shown that the origin of Feshbach resonances in interactions between ultracold rare-earth atoms with large magnetic moments result from strong scattering anisotropies. Consequently, by tuning an applied magnetic field we predict that it will be possible to observe resonances and control collisions even for atoms with zero nuclear spin. This study is the first predictions of a Feshbach resonance spectrum for rare-earth atoms.

We have investigated the effects of different short-range and long-range anisotropic potentials as well as different

isotopes on the scattering length of ultracold Dy atoms as a function of magnetic field strength. To optimize the potentials we must await experimental observations of resonances from multiple isotopic combinations.

### ACKNOWLEDGMENTS

This work is supported by grants of the AFOSR grant No. FA 9550-11-1-0243 and NSF No. PHY-1005453.

---

\* Corresponding author: skotoch@temple.edu

† Alternative address: St. Petersburg Nuclear Physics Institute, Gatchina, 188300; Department of Physics, St. Petersburg State University, 198904, Russia

- [1] B. M. Fregoso and E. Fradkin, Phys. Rev. Lett. **103**, 205301 (2009); B. M. Fregoso and E. Fradkin, Phys. Rev. B **81**, 214443 (2010).
- [2] B. M. Fregoso, K. Sun, E. Fradkin, and B. L. Lev, New J. Phys. **11**, 103003 (2009).
- [3] L. Santos and T. Pfau, Phys. Rev. Lett. **96**, 190404 (2006).
- [4] J. J. McClelland and J. L. Hanssen, Phys. Rev. Lett. **96**, 143005 (2006).
- [5] C. B. Connolly, Y. S. Au, S. C. Doret, W. Ketterle, and J. M. Doyle, Phys. Rev. A **81**, 010702(R) (2010).
- [6] Mei-Ju Lu, V. Singh, and J. D. Weinstein, Phys. Rev. A **79**, 050702(R) (2009).
- [7] M. Lu, S. H. Youn, and B. L. Lev, Phys. Rev. Lett. **104**, 063001 (2010).
- [8] M. Lu, N. Q. Burdick, S. H. Youn, and B. L. Lev, Phys. Rev. Lett. **107**, 190401 (2011).
- [9] D. Sukachev, A. Sokolov, K. Chebakov, A. Akimov, S. Kanorsky, N. Kolachevsky, and V. Sorokin, Phys. Rev. A **82**, 011405(R) (2010).
- [10] M. Lu, N. Q. Burdick, and B. L. Lev, arXiv:1202.4444v1 (2012).
- [11] J. Stuhler, A. Griesmaier, T. Koch, M. Fattori, T. Pfau, S. Giovanazzi, P. Pedri, and L. Santos, Phys. Rev. Lett. **95**, 150406 (2005).
- [12] S. Hensler, J. Werner, A. Griesmaier, P. O. Schmidt, A. Görlitz, T. Pfau, S. Giovanazzi, and K. Rzazewski, Appl. Phys. B **77**, 765 (2003).
- [13] C. I. Hancox, S. C. Doret, M. T. Hummon, L. Luo, and J. Doyle, Nature **431**, 281 (2004).
- [14] R. V. Krems, G. C. Groenenboom, and A. Dalgarno, J. Chem. Phys. **108**, 8941 (2004).
- [15] S. Kotochigova and A. Petrov, Phys. Chem. Chem. Phys. **13**, 19165 (2011).
- [16] C. Chin, R. Grimm, P. Julienne, and E. Tiesinga, Rev. Mod. Phys. **82**, 1225 (2010).
- [17] T. Köhler, K. Góral, and P.S. Julienne, Rev. Mod. Phys. **78**, 1311 (2006).
- [18] K.-K. Ni, S. Ospelkaus, M. H. G. de Miranda, A. Peér, B. Neyenhuis, J. J. Zirbel, S. Kotochigova, P. S. Julienne, D. S. Jin, and J. Ye, Science **322**, 231 (2008).
- [19] S. Giorgini, L.P. Pitaevskii, and S. Stringari, Rev. Mod. Phys. **80**, 1215 (2008); I. Bloch, J. Dalibard, and W. Zwerger, Rev. Mod. Phys. **80**, 885 (2008).
- [20] T. Kraemer, M. Mark, P. Waldburger, J. G. Danzl, C. Chin, B. Engeser, A. D. Lange, P. Pilch, A. Jaakkola, H.-C. Nägerl, and R. Grimm, Nature **440**, 315 (2006).
- [21] Yu. Ralchenko, A.E. Kramida, J. Reader, and NIST ASD Team (2011). NIST Atomic Spectra Database. Available: <http://physics.nist.gov/asd>.
- [22] A close-coupling calculation is a numerical method to find scattering solutions of a finite set of coupled radial Schrödinger equations.
- [23] G. Herzberg, *Spectra of Diatomic Molecules*, (D. Van Nostrand Company, New York, 1950).
- [24] H. Lefebvre-Brion and R. W. Field, *Perturbations in the Spectra of Diatomic Molecules*, (Academic Press, Inc, London, 1986).
- [25] J. D. Watts, J. Gauss. and R. J. Bartlett, J. Chem. Phys. **98**, 8718 (1993).
- [26] R. Santra and C.H. Greene, Phys. Rev. A **67**, 062713 (2003).
- [27] J. Werner, A. Griesmaier, S. Hensler, J. Stuhler, T. Pfau, A. Simoni, and E. Tiesinga, Phys. Rev. Lett. **94**, 183201 (2005).
- [28] G. F. Gribakin and V. V. Flambaum, Phys. Rev. A **48**, 546 (1993).
- [29] M. Kitagawa, K. Enomoto, K. Kasa, Y. Takahashi, R. Ciuryło, P. Naidon, and P. S. Julienne, Phys. Rev. A **77**, 012719 (2008).
- [30] E. Tiemann, H. Knöckel, P. Kowalczyk, W. Jastrzebski, A. Pashov, H. Salami, A. J. Ross, Phys. Rev. A **79**, 042716 (2009).